

LETTERS

Quantum signatures of chaos in a kicked top

S. Chaudhury¹, A. Smith¹, B. E. Anderson¹, S. Ghose² & P. S. Jessen¹

Chaotic behaviour is ubiquitous and plays an important part in most fields of science. In classical physics, chaos is characterized by hypersensitivity of the time evolution of a system to initial conditions. Quantum mechanics does not permit a similar definition owing in part to the uncertainty principle, and in part to the Schrödinger equation, which preserves the overlap between quantum states. This fundamental disconnect poses a challenge to quantum–classical correspondence¹, and has motivated a long-standing search for quantum signatures of classical chaos^{2,3}. Here we present the experimental realization of a common paradigm for quantum chaos—the quantum kicked top^{2,4}—and the observation directly in quantum phase space of dynamics that have a chaotic classical counterpart. Our system is based on the combined electronic and nuclear spin of a single atom and is therefore deep in the quantum regime; nevertheless, we find good correspondence between the quantum dynamics and classical phase space structures. Because chaos is inherently a dynamical phenomenon, special significance attaches to dynamical signatures such as sensitivity to perturbation^{1,5} or the generation of entropy⁶ and entanglement^{7,8}, for which only indirect evidence has been available^{9–11}. We observe clear differences in the sensitivity to perturbation in chaotic versus regular, non-chaotic regimes, and present experimental evidence for dynamical entanglement as a signature of chaos.

In classical mechanics, the state of a physical system is specified by a set of dynamical variables—for example, the position and momentum of a point particle—whose values define a point in phase space. Regular motion is associated with periodic orbits in phase space, whereas chaos is characterized by complex, aperiodic trajectories that diverge exponentially as a function of initial separation. This description of states and time evolution is fundamentally incompatible with quantum mechanics, where conjugate observables such as position and momentum cannot take on well-defined values at the same time. However, it is still possible to represent a quantum state in phase space, in the form of a delocalized quasi-probability distribution whose evolution is governed by the Schrödinger equation¹². This suggests an experiment in which one prepares an initial minimum uncertainty state centred on a point in phase space, subjects it to a desired evolution, measures the quantum state at successive points in time, and observes the degree to which the dynamically evolving quantum phase space distribution reflects the classical phase space structures. Experiments of this type can be simulated with classical waves³, but are very challenging for true quantum systems because of the overhead involved in state preparation, control and reconstruction. Quantum versions that accomplish several of the steps have been performed with cold atoms in laser standing waves^{13,14}, and in this Letter we complete the entire programme by including full quantum state reconstruction and visualizing the dynamics via complete phase space distributions. Placing the emphasis on dynamics complements the much larger body of experimental work on energy level statistics in a broad range of physical systems^{15–17}.

The experimental tools required to study quantum chaos directly in phase space have recently become available for the physical system

consisting of the spin angular momentum of a single ¹³³Cs atom in the $F = 3$ hyperfine ground state^{18–20}. To take advantage of this, we have implemented a very popular model system known as the ‘kicked top’, consisting of a spin F whose dynamics is governed by a periodic Hamiltonian:

$$H = \hbar p F_y \sum_{n=0}^{\infty} f(t - n\tau) + \hbar \frac{\kappa}{2F\tau} F_x^2 \quad (1)$$

In the simplest case, the kick f is a δ -function, and each period of the classical evolution breaks down into a rotation about the y axis by a fixed angle p , followed by a twist (a rotation about the x axis by an angle proportional to F_x). The parameter κ determines the degree to which the dynamics are regular or chaotic. In our experiment, the rotation is performed by applying a short magnetic field pulse, whereas the twist is induced by the a.c. Stark shift (light shift) from a laser field tuned near the D1 resonance at 895 nm (ref. 18). Because the magnitude of the spin is conserved, phase space is a spherical surface on which each point represents a particular orientation of the spin, and the classical evolution can be visualized by a stroboscopic plot showing the state at times $t = n\tau$. Figure 1 shows such a phase space plot for our kicked top, with parameters $p = 0.99$ and $\kappa = 2.0$. We see immediately that the phase space is mixed, with one large island of regular motion in the $F_y < 0$ hemisphere, two smaller islands in the $F_y > 0$ hemisphere, and a sea of chaos almost everywhere else.

To visualize a quantum state of the kicked top in phase space, one can expand it in a basis of spin-coherent states $|\theta, \phi\rangle$, which are minimum uncertainty states with maximum projection in the directions

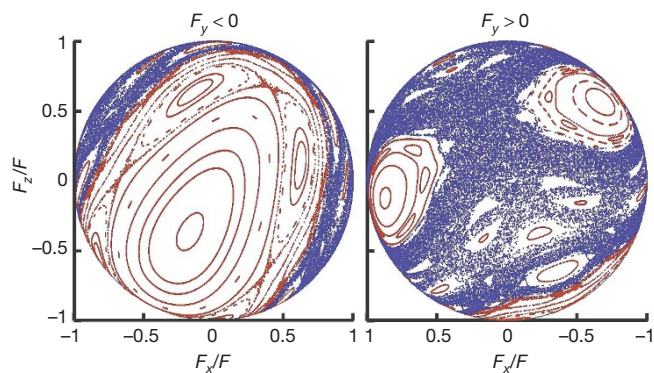


Figure 1 | Stroboscopic phase space plot for a classical kicked top.

Trajectories are obtained by integrating the classical equations of motion and plotting the position of the spin after each kick. Depending on the starting point, states follow regular orbits (red), or move along chaotic trajectories (blue). Motion across the boundaries between regular and chaotic regions is classically forbidden. For this plot $p = 0.99$ and $\kappa = 2.0$, resulting in a mixed phase space that contains both regular islands of various sizes and a sea of chaos. The $F_y < 0$ and $F_y > 0$ hemispheres are shown separately, respectively left and right.

¹College of Optical Sciences, University of Arizona, Tucson, Arizona 85721, USA. ²Department of Physics and Computer Science, Wilfrid Laurier University, Waterloo, Ontario N2L 3C5, Canada.

given by the polar and azimuthal angles (θ, ϕ) and thus the closest quantum approximation to a classical spin. This produces the Husimi quasi-probability distribution, $Q(\theta, \phi) = (2F + 1) \langle \theta, \phi | \rho | \theta, \phi \rangle / 4\pi$, where ρ is the density operator for the quantum state (pure or statistical mixture)²¹. $Q(\theta, \phi)$ is a normalized, everywhere positive function that comes as close as possible to a classical probability distribution in phase space.

We use as a starting point for our kicked-top experiments an ensemble of laser-cooled Cs atoms prepared by optical pumping in a desired spin-coherent state $\rho_0 \approx |\theta, \phi\rangle\langle\theta, \phi|$. In a given run of the experiment, each member of the ensemble is subjected to n periods of the kicked-top Hamiltonian, and the entire density operator for the final state is experimentally reconstructed¹⁹. The process is repeated for $0 \leq n \leq 40$, in order to build up a stroboscopic record $\{\rho_n\}$ for the evolving quantum state. Finally, we carry out the entire procedure for a series of initial states. To obtain a visual quantum–classical comparison, we convert each data set $\{\rho_n\}$ into Husimi distributions to obtain a ‘stop-motion movie’ of the evolution of the state. Figure 2A shows selected frames from a movie obtained for an initial spin-coherent state centred on the stable island near $F_x/F = 1$ in the $F_y > 0$ hemisphere. Successive frames clearly show the phenomenon of dynamical tunnelling, wherein the quantum system oscillates between two regions of phase space even though motion through the chaotic sea is classically forbidden^{13,14}. The observed tunnelling period is in good agreement with a prediction based on decomposition of the initial state into Floquet eigenstates (Supplementary

Information). It is also clear that the tunnelling oscillation dephases after roughly one period. This is a sign of imperfections in our experiments, mainly a 5% variation in κ due to laser intensity variation across the ensemble, decoherence induced by spontaneous light scattering (~ 1 photon per 15 kicks), and background magnetic fields. Our data are in good quantitative agreement with a full master equation calculation that includes these imperfections.

An additional, useful visualization of data of the type displayed in Fig. 2 can be achieved by averaging the Husimi distribution over many cycles. The result is a single plot showing the parts of phase space accessible from a given initial state. Figure 2C shows 40-period averages for three initial states, which together illustrate the remarkable degree to which our quantum kicked top reflects the boundaries between regular and chaotic regions in classical phase space. Although this is to be expected for systems in the mesoscopic regime, it is somewhat surprising that our deeply quantum mechanical spin should do so.

In recent years, much attention has been directed towards dynamical signatures of chaos in quantum systems. One candidate is the sensitivity to perturbation, which can be quantified by the decay in overlap between quantum states evolving according to two slightly different Hamiltonians, and which can potentially reflect the classical Lyapunov exponent²². The spin in our experiment is too small for the overlap to undergo exponential decay, but different sensitivities to perturbation should still be reflected in the decay of the purity of the spin density operator, as each spin evolves with a slightly different value of κ , and is coupled to the environment through light scattering.

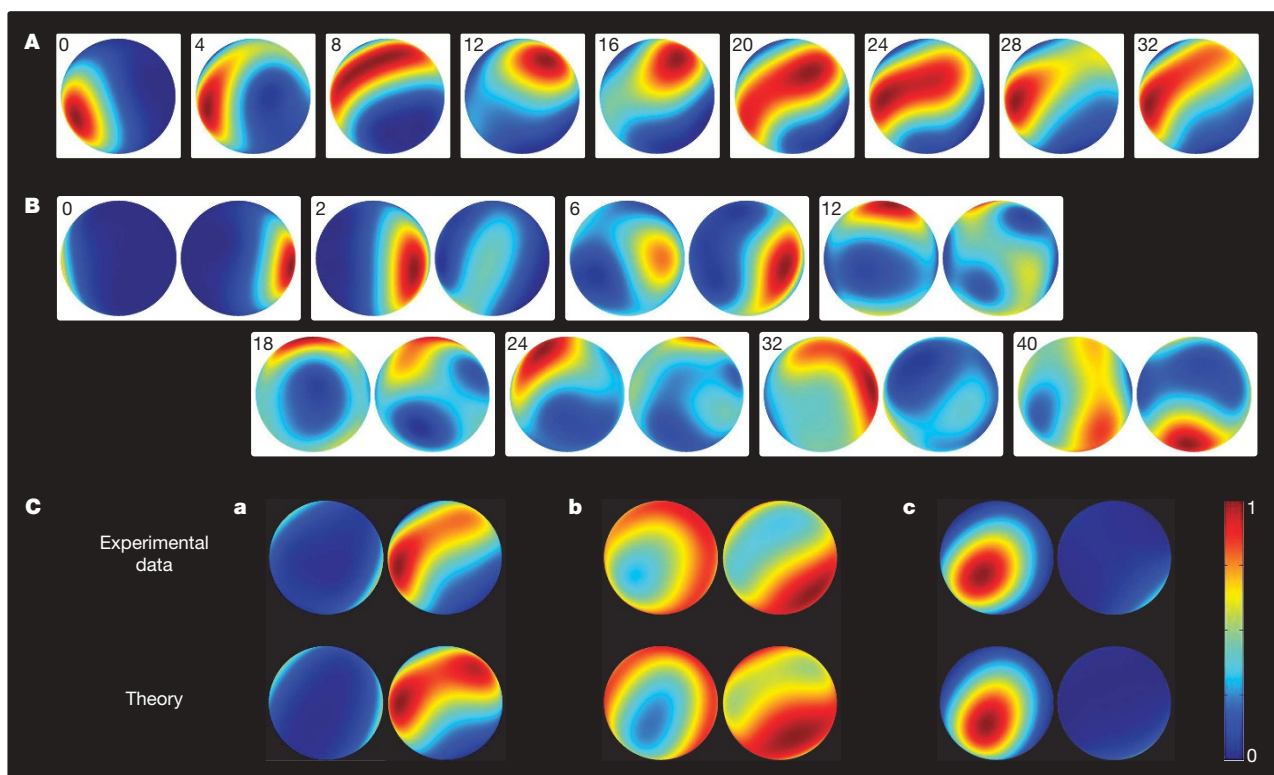


Figure 2 | Quantum phase space (Husimi) distributions for a quantum kicked top. Stroboscopic illustration of dynamical evolution, showing selected experimental snapshots from the first 40 periods of the kicked-top Hamiltonian. The period number is indicated in each frame. **A**, The initial state is a spin-coherent state centred at $F_x/F = 0.70$, $F_y/F = 0.70$, $F_z/F = -0.16$, where it is mostly contained within the boundaries of the lower of the pair of islands in the $F_y > 0$ hemisphere of Fig. 1. The state undergoes roughly 1.5 periods of dynamical tunnelling before coherence is lost. The state is almost entirely confined to the $F_y > 0$ hemisphere, which is the only one shown. **B**, The initial state is a spin-coherent state centred at $F_x/F = -0.94$, $F_y/F = 0.31$, $F_z/F = -0.16$, where it is mostly contained within the chaotic sea. The state spreads into the chaotic regions but generally avoids the regular islands. Both hemispheres are shown.

C, 40-period averages of evolving Husimi distributions. **a–c**, The initial states are spin-coherent states centred at **a**, $F_x/F = 0.70$, $F_y/F = 0.70$, $F_z/F = -0.16$ (island in the $F_y > 0$ hemisphere, same as **A**), at **b**, $F_x/F = -0.94$, $F_y/F = 0.31$, $F_z/F = -0.16$ (in the chaotic sea, same as **B**), and at **c**, $F_x/F = 0$, $F_y/F = -0.99$, $F_z/F = -0.16$ (large island in the $F_y < 0$ hemisphere). The upper data set is the observation from experiments, while the lower data set is the prediction of a full theoretical model taking into account decoherence and κ variation. In combination, the quantum phase space distributions reflect the classical phase space structures of Fig. 1 with remarkable fidelity. To enhance contrast, the Husimi distribution in each image has been rescaled to fit the interval $[0, 1]$. Each quantum state is experimentally reconstructed with a fidelity of $\sim 90\%$.

Figure 3 shows the experimentally measured state purity, $\text{Tr}[\rho^2]$, as a function of period number, for two different initial states. As predicted, the purity decays at very different rates in regular and chaotic regions.

For systems with multiple degrees of freedom, it has been argued that classical chaos is linked to the dynamical generation of entanglement in the quantum system^{23,24}. Our atomic spin is the sum of electron and nuclear spins, $\mathbf{F} = \mathbf{S} + \mathbf{I}$. It is therefore natural to test if the entanglement generated between the two is a reliable signature of chaos. Here we use the linear entropy $S_{\text{LE}} = 1 - \text{Tr}[\rho_e^2]$ as our entanglement measure, where ρ_e is the reduced density operator for the electron spin. This is reasonable as long as the overall state is nearly pure. In our experiment, S_{LE} reaches steady state after just a few kicks (Supplementary Information), and the 40-period average therefore serves as a convenient and robust measure of the entanglement generated by the dynamics. Figure 4 shows a significant dip in $\langle S_{\text{LE}} \rangle$ and correspondingly less entanglement generation for initial states localized in regular regions compared to those in the chaotic sea. This is (to our knowledge) the first experimental evidence that the purely quantum property of entanglement is a good signature of classical chaos. Note that whereas the signature is very clear for initial states in the large regular island in the $F_y < 0$ hemisphere, it is less apparent for states located on the small island in the $F_y > 0$ hemisphere. This loss in contrast occurs because the latter become entangled by dynamical tunnelling, and is therefore linked to the deeply quantum nature of our small spin. Contrast is further reduced by the sensitivity of tunnelling to κ variations and decoherence, which is apparent from the difference between our perturbation-free and full models (Supplementary Information). Tunnelling will be suppressed for much larger spins, and it is reasonable to assume that the distinction between regular and chaotic regions will be more universal in that regime.

Our laboratory realization of the kicked top with atomic spins points the way to further studies of quantum chaos in the time domain. We are currently working to extend our control and measurement tools to the entire hyperfine ground manifold of the Cs atom²⁵, which will provide access to the full state space for the coupled electron–nuclear spins. Besides increasing the size of state space by more than a factor of two, this will offer a more powerful platform for the study of entanglement as a quantum signature of chaos²⁶. To reach the semiclassical limit of very large spins, one can in principle implement a kicked-top Hamiltonian for the collective spin of an atomic ensemble, with the twisting interaction induced either by ultracold collisions²⁷, or by coupling the spins to a shared mode of a quantized electromagnetic field²⁸.

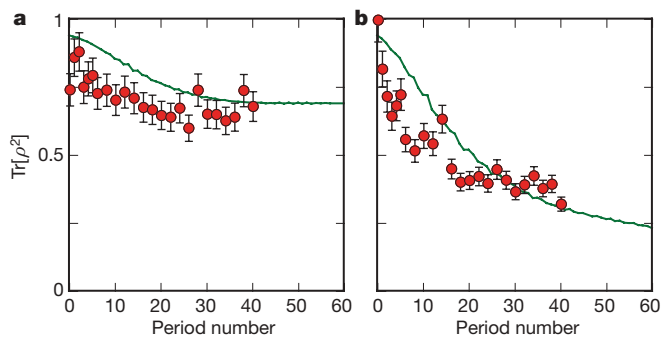


Figure 3 | Sensitivity to perturbation as a quantum signature of chaos. The purity of the spin density operator, $\text{Tr}[\rho^2]$, shown as a function of the period number. **a**, Initial state localized on the large island in the $F_y < 0$ hemisphere (same data set as in Fig. 2C, c). **b**, Initial state localized in the sea of chaos (same data set as in Fig. 2C, b). Red circles are experimental data and the green lines are the predictions of a full model. As expected, perturbations, in the form of decoherence and κ variation across the ensemble, reduce the purity much faster for a state in the chaotic sea. Experimental error bars, ± 1 s.d.

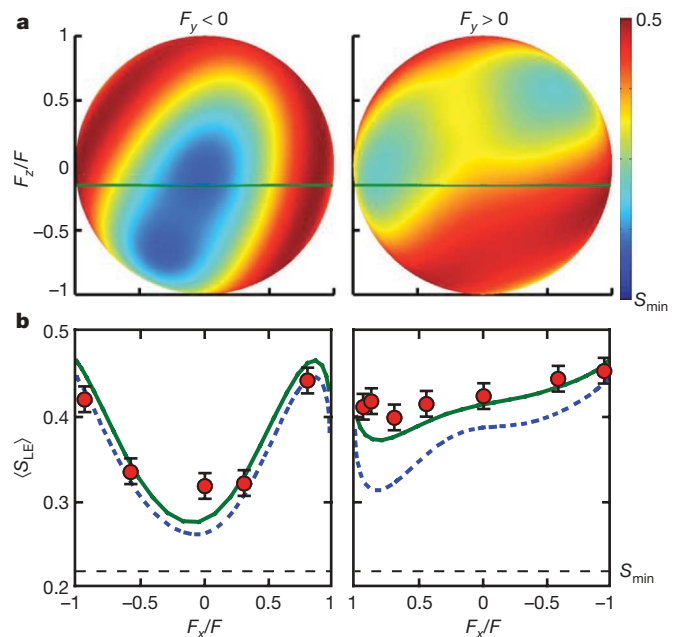


Figure 4 | Entanglement as a quantum signature of chaos. Entanglement between the electron and nuclear spins is quantified by the linear entropy, $S_{\text{LE}} = 1 - \text{Tr}[\rho_e^2]$, of the electron reduced density operator. It is averaged over 40 periods of the kicked-top Hamiltonian, and shown as a function of the centre of the initial spin coherent state $|\theta, \phi\rangle$. **a**, Theoretical prediction for Schrödinger evolution, corresponding to an ideal situation without perturbations (no decoherence or κ variation). Colours indicate the value of $\langle S_{\text{LE}} \rangle$. **b**, Experimental measurements performed for states lying along the green cross-section in **a**. Also shown are the predictions of a full model (solid green line) and the perturbation free model (dashed blue line) used in **a**. The black dashed line is the linear entropy of a minimally entangled pure state in the $F = 3$ manifold. A marked contrast in dynamically generated entanglement can be seen between regular and chaotic regions. Experimental error bars, ± 1 s.d.

Ultimately, this could allow experiments to address some of the most important outstanding questions related to quantum–classical correspondence, such as how to recover classical (chaotic) dynamics in open quantum systems subject to decoherence²² or weak measurement²⁹.

METHODS SUMMARY

We prepare a spin ensemble by capturing and laser cooling $\sim 10^7$ Cs atoms in a magneto-optical trap and optical molasses. The atoms are released into free fall, and optically pumped into an $F = 3$ spin-coherent state with respect to a fixed axis. A set of precision coils driven by arbitrary waveform generators apply time-dependent magnetic fields in a bandwidth of ~ 200 kHz, and generate fast and accurate rotations through the magnetic interaction $g_F \mu_B \mathbf{B} \cdot \mathbf{F}$, where g_F is the Landé g factor for the spin F and μ_B is the Bohr magneton. We use magnetic field pulses to prepare spin-coherent states along desired directions, and to perform the rotation in the kicked-top Hamiltonian. The continuous twist is induced by the a.c. Stark shift in a linearly polarized, monochromatic laser field, leading to an effective ground state Hamiltonian of the form $\hbar \zeta F_x^2$ (ref. 18). In our experiment the magnetic kick duration is 17 μs , the peak Larmor frequency is 15 kHz, the twisting strength $\zeta = 2\pi \times 533$ Hz, and the kicked-top period is $\tau = 100$ μs for $\kappa = 2.0$. The finite duration of the magnetic kick causes overlap of the rotation and twisting parts of the evolution, but this does not significantly alter the character of the dynamics and is easily taken into account in the equations of motion. The rotation, $p = 0.99$, is chosen to maximize the size of the islands in the $F_y > 0$ hemisphere, and to allow a spin coherent state to be contained mostly within one of these.

Following n periods of the kicked-top Hamiltonian, the information needed to reconstruct the final spin density operator with a fidelity of $\sim 90\%$ is acquired during a single 2-ms phase of continuous weak optical measurement and dynamical control. Details regarding nonlinear spin dynamics, quantum control and quantum state reconstruction, and the theoretical modelling of spin dynamics, can be found in previous work published by our group^{18,19,30}.

Received 16 June; accepted 6 August 2009.

1. Peres, A. *Quantum Theory: Concepts and Methods* (Springer, 1995).
2. Haake, F. *Quantum Signatures of Chaos* (Springer, 2001).
3. Stöckmann, H.-J. *Quantum Chaos: An Introduction* (Cambridge Univ. Press, 1999).
4. Haake, F., Kus, M. & Scharf, R. Classical and quantum chaos for a kicked top. *Z. Phys. B* **65**, 381–395 (1987).
5. Peres, A. Stability of quantum motion in chaotic and regular systems. *Phys. Rev. A* **30**, 1610–1615 (1984).
6. Zurek, W. H. & Paz, J. P. Decoherence, chaos, and the Second Law. *Phys. Rev. Lett.* **72**, 2508–2511 (1994).
7. Furuya, K., Nemes, M. C. & Pellegrino, G. Q. Quantum dynamical manifestation of chaotic behavior in the process of entanglement. *Phys. Rev. Lett.* **80**, 5524–5527 (1998).
8. Jalabert, R. A. & Pastawski, H. M. Environment-independent decoherence rate in classically chaotic systems. *Phys. Rev. Lett.* **86**, 2490–2493 (2001).
9. Weinstein, Y. S., Lloyd, S., Emerson, J. & Cory, D. G. Experimental implementation of the quantum baker's map. *Phys. Rev. Lett.* **89**, 157902 (2002).
10. Ryan, C. A., Emerson, J., Poulin, D., Negrevergne, C. & Laflamme, R. Characterization of complex quantum dynamics with a scalable NMR information processor. *Phys. Rev. Lett.* **95**, 250502 (2005).
11. Andersen, M. F., Kaplan, A. & Davidson, N. Echo spectroscopy and quantum stability of trapped atoms. *Phys. Rev. Lett.* **90**, 023001 (2003).
12. Lee, H. W. Theory and application of the quantum phase-space distribution functions. *Phys. Rep.* **259**, 147–211 (1995).
13. Steck, D. A., Oskay, W. H. & Raizen, M. G. Observation of chaos-assisted tunnelling between islands of stability. *Science* **293**, 274–278 (2001).
14. Hensinger, W. K. *et al.* Dynamical tunnelling of ultracold atoms. *Nature* **412**, 52–55 (2001).
15. Weidenmüller, H. A. & Mitchell, G. E. Random matrices and chaos in nuclear physics: nuclear structure. *Rev. Mod. Phys.* **81**, 539–589 (2009).
16. Blümel, R. & Reinhardt, W. P. *Chaos in Atomic Physics* (Cambridge Univ. Press, 1997).
17. Alhassid, Y. The statistical theory of quantum dots. *Rev. Mod. Phys.* **72**, 895–968 (2000).
18. Chaudhury, S. *et al.* Quantum control of the hyperfine spin of a Cs atom ensemble. *Phys. Rev. Lett.* **99**, 163002 (2007).
19. Smith, G. A., Silberfarb, A., Deutsch, I. H. & Jessen, P. S. Efficient quantum-state estimation by continuous weak measurement and dynamical control. *Phys. Rev. Lett.* **97**, 180403 (2006).
20. Ghose, S., Stock, R., Jessen, P., Lal, R. & Silberfarb, A. Chaos, entanglement, and decoherence in the quantum kicked top. *Phys. Rev. A* **78**, 042318 (2008).
21. Agarwal, G. S. Relation between atomic coherent-state representation, state multipoles, and generalized phase-space distributions. *Phys. Rev. A* **24**, 2889–2896 (1981).
22. Habib, S., Shizume, K. & Zurek, W. H. Decoherence, chaos, and the correspondence principle. *Phys. Rev. Lett.* **80**, 4361–4365 (1998).
23. Prosen, T. Chaos and complexity of quantum motion. *J. Phys. A* **40**, 7881–7918 (2007).
24. Jacquod, Ph & Petitjean, C. Decoherence, entanglement and irreversibility in quantum dynamical systems with few degrees of freedom. *Adv. Phys.* **58**, 67–196 (2009).
25. Merkel, S. T., Jessen, P. S. & Deutsch, I. H. Quantum control of the hyperfine-coupled electron and nuclear spins in alkali-metal atoms. *Phys. Rev. A* **78**, 023404 (2008).
26. Trail, C. M., Madhok, V. & Deutsch, I. H. Entanglement and the generation of random states in the quantum chaotic dynamics of kicked coupled tops. *Phys. Rev. E* **78**, 046211 (2008).
27. Micheli, A., Jaksch, D., Cirac, J. I. & Zoller, P. Many-particle entanglement in two-component Bose-Einstein condensates. *Phys. Rev. A* **67**, 013607 (2003).
28. Takeuchi, M. *et al.* Spin squeezing via one-axis twisting with coherent light. *Phys. Rev. Lett.* **94**, 023003 (2005).
29. Bhattacharya, T., Habib, S. & Jacobs, K. Continuous quantum measurement and the emergence of classical chaos. *Phys. Rev. Lett.* **85**, 4852–4855 (2000).
30. Silberfarb, A., Jessen, P. S. & Deutsch, I. H. Quantum state reconstruction via continuous measurement. *Phys. Rev. Lett.* **95**, 030402 (2005).

Supplementary Information is linked to the online version of the paper at www.nature.com/nature.

Acknowledgements We thank I. H. Deutsch and P. Jacquod for discussions. This work was supported by the National Science Foundation (grant no. 0653631) and the Office of Naval Research (grant no. N00014-05-1-420). S.G. was supported by an NSERC Discovery grant.

Author Contributions All authors contributed extensively to this work.

Author Information Reprints and permissions information is available at www.nature.com/reprints. Correspondence and requests for materials should be addressed to P.S.J. (poul.jessen@optics.arizona.edu).